NOTE

Magnetic Resonance in Medicine 00:00–00 (2015)

Handheld Electromagnet Carrier for Transfer of Hyperpolarized Carbon-13 Samples

Hong Shang,[1,2] Timothy Skloss,[3] Cornelius von Morze,[1] Lucas Carvajal,[1] Mark Van Criekinge,[1] Eugene Milshteyn,[1,2] Peder E. Z. Larson,[1,2] Ralph E. Hurd,[3] and Daniel B. Vigneron[1,2]*

Purpose: Hyperpolarization of carbon-13 (^{13}C) nuclei by dissolution dynamic nuclear polarization increases signal-to-noise ratio (SNR) by >10,000-fold for metabolic imaging, but care must be taken when transferring hyperpolarized (HP) samples from polarizer to MR scanner. Some ^{13}C substrates relax rapidly in low ambient magnetic fields. A handheld electromagnet carrier was designed and constructed to preserve polarization by maintaining a sufficient field during sample transfer.
Methods: The device was constructed with a solenoidal electromagnet, powered by a nonmagnetic battery, holding the HP sample during transfer. A specially designed switch automated deactivation of the field once transfer was complete. Phantom and rat experiments were performed to compare MR signal enhancement with or without the device for HP [^{13}C]urea and [1-^{13}C]pyruvate.
Results: The magnetic field generated by this device was tested to be >50 G over a 6-cm central section. In phantom and rat experiments, [^{13}C]urea transported via the device showed SNR improvement by a factor of 1.8–1.9 over samples transferred through the background field.
Conclusion: A device was designed and built to provide a suitably high yet safe magnetic field to preserve hyperpolarization during sample transfer. Comparative testing demonstrated SNR improvements of approximately two-fold for [^{13}C]urea while maintaining SNR for [1-^{13}C]pyruvate. **Magn Reson Med 000:000–000, 2015.** © **2015 Wiley Periodicals, Inc.**

Key words: hyperpolarized carbon-13 MRI/MRSI; dynamic nuclear polarization; low magnetic field; T1 relaxation; scalar coupling; urea

INTRODUCTION

Hyperpolarized carbon-13 (HP ^{13}C) MRI with dissolution dynamic nuclear polarization (DNP) (1) has recently been shown to provide biologic information on previously inaccessible aspects of metabolic processes by detecting endogenous, nontoxic ^{13}C-labeled probes to monitor enzymatic conversions through key biochemical pathways (2–4). Because both spatial and chemical information are encoded, this new molecular imaging modality allows simultaneous detection of multiple biologic compounds and metabolic products with sensitivity enhancements of >10,000-fold (1). The recently completed phase 1 clinical trial conducted at the University of California, San Francisco, demonstrated the safety and feasibility of HP ^{13}C-pyruvate MRI in prostate cancer patients without any dose-limiting or other notable toxicities (5).

Some HP ^{13}C substrates can lose polarization extremely quickly in low magnetic field when they are transferred between the polarizer and the MR scanner, reducing the SNR. For example, scalar coupling between fast-relaxing quadrupolar ^{14}N and ^{13}C results in rapid loss of polarization of [^{13}C]urea (6). Although most in vivo HP ^{13}C MRI studies have focused on probing metabolism using metabolically active substrates (7), several studies have shown that metabolically inactive agents such as [^{13}C]urea can be applied to angiography or perfusion imaging (8,9). HP [^{13}C]urea for perfusion MRI has advantages over conventional gadolinium-containing (paramagnetic) contrast agents, including direct proportionality of signal to concentration, inherently high contrast-to-noise ratio due to the absence of background signal, and an excellent safety profile potentially benefitting studies in patients who are currently excluded from contrast imaging studies. In addition, [^{13}C]urea can be copolarized with [1-^{13}C]pyruvate for combined perfusion and metabolic imaging (10,11). Urea is a safe, endogenous compound with normally high concentrations in vivo (typically 1–10 mM, and much higher in the renal medullary interstitium), low toxicity, and neutral pH, as well as the key MR properties of long T_1 relaxation time and high polarization by DNP. Recent studies have also demonstrated the ability of HP [^{13}C]urea to identify changes in urea transport and concentration in the kidney (12).

In previous studies, this loss of polarization of [^{13}C]urea during sample transfer has been addressed by carrying a permanent magnet next to the HP sample, or at the molecular level by secondary labeling with ^{15}N (6,13). However, the cost of [^{13}C,^{15}N$_2$]urea is about five times higher than [^{13}C]urea. Furthermore, J-coupling in [^{13}C,^{15}N$_2$]urea splits the ^{13}C NMR resonance peak into a triplet, thus lowering the signal amplitude and potentially confounding quantitation. The permanent magnet method raises safety concerns, because the magnet could cause harm by flying into the scanner. In addition, permanent magnets provide

[1]Department of Radiology and Biomedical Imaging, University of California, San Francisco, San Francisco, California, USA.
[2] The UC Berkeley - UCSF Graduate Program in Bioengineering, California, USA.
[3]GE Healthcare, USA.

Grant sponsor: University of California, San Francisco Hyperpolarized MRI Technology Resource Center; Grant sponsor: National Institutes of Health; Grant numbers: P41-EB013598, R01-EB013427, K01-DK099451; Grant sponsor: GE Healthcare; Grant number: R01-EB017449.

*Correspondence to: Daniel B. Vigneron, 1700 4th Street, Byers Hall Suite 102F, MC 2512, San Francisco, CA 94158-2330.
E-mail: dan.vigneron@ucsf.edu

Received 5 December 2014; revised 18 January 2015; accepted 24 January 2015
DOI 10.1002/mrm.25657
Published online 00 Month 2015 in Wiley Online Library (wileyonlinelibrary.com).

nonuniform fields and are impractical for large samples. To address these limitations, we constructed and tested a new electromagnet carrier device to provide a suitable and relatively uniform magnetic field for the safe transfer of HP samples for ^{13}C MR studies.

THEORY

Spin-lattice relaxation depends on several independent mechanisms, including interactions with paramagnetic centers and scalar coupling between fast-relaxing quadrupolar nuclei, which cause faster relaxation when the magnetic field decreases. Quadrupolar nuclei with spin >1/2 (eg, ^{14}N) have very short T_1 values. The scalar coupling of ^{13}C to ^{14}N provides a relaxation mechanism for ^{13}C as ^{14}N is undergoing very rapid T_1 relaxation. The scalar coupling relaxation rate can be calculated by

$$R_{SC} = \frac{8\pi^2 J^2}{3} I(I+1) \frac{T_1}{1 + (\Delta\omega)^2 T_1^2}, \quad [1]$$

where R_{sc} is the scalar coupling relaxation rate, J is the scalar coupling constant in Hertz, I is the spin quantum number of the coupled nucleus ($I_{14N} = 1$), T_1 is the spin-lattice relaxation time of the quadrupolar nucleus (^{14}N), and $\Delta\omega = \omega_{13c} - \omega_{14N}$ is the difference in Larmor frequencies of coupled nuclei ^{13}C and ^{14}N. For this mechanism to be effective, the Larmor frequencies of these two nuclei must be very close. This condition is met at low magnetic fields (eg, during HP sample transfer), although it may also occur at high fields (eg, for ^{13}C [15.087 MHz] and ^{79}Br [15.023 MHz] at 1.41 T) (14). One approach to reduce the scalar coupling relaxation mechanism is to increase the external magnetic field.

METHODS

Simulation and Background Field Measurements

The ambient magnetic field through which the HP samples were transferred was measured with a three-axis Hall effect magnetometer (THM 7025; Metrolab Technology SA, Geneva, Switzerland), as shown in Figure 1A. R_{sc} was estimated as a function of magnetic field based on Equation 1 according to the parameters described in Chiavazza et al. (6), including $T_1 = 1.0 \pm 0.1$ ms and $J = 14.5 \pm 0.1$ Hz (Fig. 1B). Assuming a piece-wise constant relaxation rate along the path and constant transfer velocity over a 6s transfer, the signal decay curve can be estimated along this path (Fig. 1C).

By adding a magnetic field offset of 50 G (in the vertical direction) in simulation, this scalar coupling relaxation mechanism can be significantly reduced as shown in Figure 1B, resulting in a 1.83-fold signal improvement at the end of the path as shown in Fig. 1C. This field strength specification was used for the design of this device to provide an adequate magnetic field to maintain a long T_1 for HP samples during transfer.

Hardware

The electromagnet carrier device was designed to provide a suitable magnetic field for the safe transfer of HP samples. The key part of the device is a solenoid with a current of 0.5 A powered by a nonmagnetic battery to generate a relatively uniform magnetic field of >50 G over a 6-cm longitudinal section. The size of the solenoid was customized for the specific 3-mL and 5-mL syringes (BD, Franklin Lakes, New Jersey, USA) commonly used for preclinical HP ^{13}C studies. The inner diameter and the length were designed to be 1.65 cm and 7.9 cm, respectively. The gauge of the wire (22 AWG) and number of layers (six) were chosen based on the desired field of 50 G, resulting in a total of 727 turns.

The circuit is shown in Figure 2A. A single-cell (3.7 V), 500-mAH lithium-ion polymer battery (E-flite; Horizon Hobby, Champaign, Illinois, USA) composed of nonmagnetic materials powered the magnetic field. The device can be safely carried into the 3 T MRI scanner room and turned off there. The current was activated by depressing the default-open, push-button momentary switch. When the button was released, the current was turned off automatically. The design of the switch ensures that the device can be safely operated in the scanner room, covering the entire sample transfer path and thus minimizing the loss of polarization. An LED was installed to indicate when the device was activated. The battery can provide stable current for at least 1 hour of continuous use. The sample transfer duration is <10 s, so one battery charge can last for hundreds of hyperpolarization experiments.

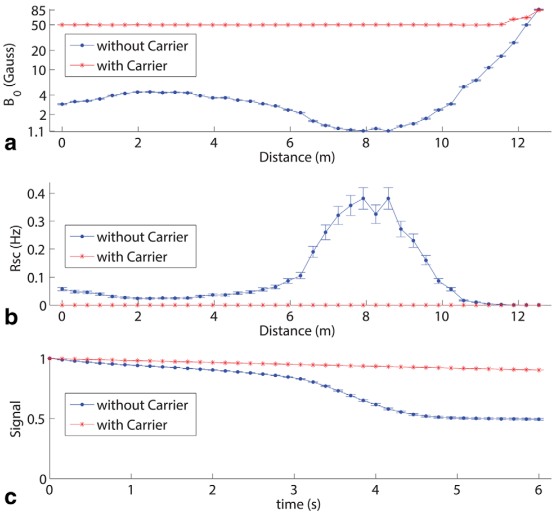

FIG. 1. **A:** Measured ambient magnetic field magnitudes along the sample transfer path (without carrier, blue lines) and simulated field magnitude with 50 G added along the vertical direction (with carrier, red lines). The *y* axis (B_0) is displayed with a log scale. The distance of 15.4 m corresponds to the center of the MR scanner and 0 m corresponds to the location of the DNP polarizer. The range of distance (0–13.4 m) corresponds to the part of the sample transfer path where the device was used. **B:** Estimated scalar coupling relaxation rate of HP [^{13}C]urea along the path corresponding to the two different fields. **C:** Estimated signal decay curve along the path assuming piece-wise constant relaxation rate and constant transfer speed within 6 s.

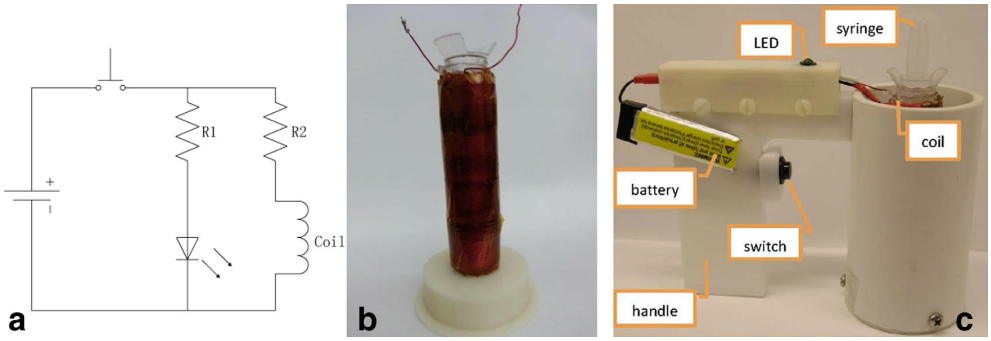

FIG. 2. Hardware design of electromagnet carrier device. **A:** Circuit diagram. Resistance of the coil = 2.9 Ω, R1 = 833 Ω, R2 = 4.4 Ω. A nonmagnetic, 500-mAH lithium-ion polymer battery supplies 3.7 V and a current of 0.5 A in the coil (current in the LED = 2.1 mA). The switch is a default-open, push-button momentary switch. **B:** Photograph of the solenoid inside. **C:** Photograph of the entire device.

The device (Fig. 2C) was constructed using a combination of custom three-dimensional (3D)-printed parts and commercially available parts meeting the design criteria for performance, nonmagnetic materials, and durability. The housing was built with strength to withstand drops to the floor, and the shape was designed for ease of carrying and standing upright. The switch was trigger-mounted to enable easy depression, holding and releasing of the button. The battery was attached on the surface of the device in a manner allowing easy replacement or charging. The inner diameter of the solenoid-encompassed sample chamber closely fits the syringes, which are quickly guided through a conical opening on top of the coil, as shown in Figure 2B.

Magnetic Field Measurements

The strength, stability, and uniformity of the device magnetic field were simulated and measured. The magnetic field strength along the central axis was first simulated based on the Biot-Savart Law. Assuming the magnetic field in the solenoid is uniform, the field strength along the central axis approximates the field inside the solenoid. The same magnetometer described above was used to measure the field inside the solenoid. The solenoid for the actual device had a smaller inner diameter, which was customized for the sample size. This smaller size was too narrow for the probe of the magnetometer. Therefore, a prototype solenoid of larger size was constructed to test the accuracy of the field simulation in comparison with the measured results.

HP MR Phantom Experiments

Experiments were performed to test the effect of the device on HP [^{13}C]urea and copolarization of [^{13}C]urea and [1-^{13}C]pyruvate. Dissolution DNP was performed with a HyperSense polarizer (Oxford Instruments, Oxford, UK) operating at 1.3 K and 3.35 T, using previously described methods, generating 4.5 mL of the 100 mM HP solution (11). MR experiments were performed on a 3 T clinical MRI scanner (GE Healthcare, Waukesha, Wisconsin, USA) with a broadband radiofrequency amplifier. Custom built, dual-tuned mouse birdcage coils (l = 8 cm, d = 5 cm) were used for radiofrequency transmission and signal reception. The radiofrequency transmit gain was calibrated with a ^{13}C-enriched urea phantom with similar size and similar location as the HP phantom.

After dissolution, the HP sample was divided into two equally apportioned syringes, and both were carried to the scanner at the same speed along the same path. One was transferred in the ambient field, while the other was transferred with this device. The device was turned on during DNP dissolution and kept activated throughout the transfer from DNP polarizer to MR scanner. It was deactivated approximately 2 m away from the center of the MR scanner, where the fringe field is already sufficiently large. The device was held vertically during transfer such that the magnetic field from this device was added to the fringe field instead of potentially cancelling each other. The sample transfer took approximately 6 s.

The solutions were then injected into two fixed syringe reservoirs already lying inside the coil, oriented along the longitudinal direction. The signal of these two samples was then acquired together with one pulse sequence and approximately the same local B_0 and B_1 fields. In this manner, the differences in signal between the samples transferred with and without the device were calculated from the same experiment, while controlling for any variations in initial polarization, total amount of sample, and transfer duration. Another control group experiment was performed with the same imaging methods, but both samples were transferred without the device. The urea-only experiment and control group experiment were each repeated four times, and the copolarization experiment was repeated five times.

For the urea-only tests, the axial images were acquired with single-shot echo planar imaging (EPI) readout, with no localization along the longitudinal direction, using the following parameters: flip angle = 90°; echo time (TE) = 100 ms; repetition time (TR) = 250 ms; matrix size = 20 × 20; field of view = 10 × 10 cm. For urea and pyruvate copolarization tests, a dynamic one-dimensional MR spectroscopic imaging sequence was used with hard pulse excitation (0.5 ms duration),

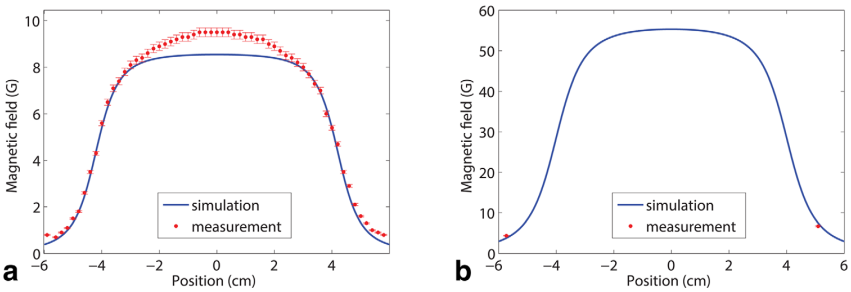

FIG. 3. Simulated (blue line) and measured (red dots) magnetic field distribution in the prototype solenoid with larger diameter (A) and the solenoid used in the device (B). Error of measurement (shown as red error bars) were determined from the accuracy of the magnetometer. The measured field distribution was not available for the solenoid in the device because its size is smaller than the probe of the magnetometer, but the calculation demonstrated a field of greater than 50 G over the central 6 cm.

double spin echo refocusing, and symmetric EPI readout (15). Spatial encoding was only applied along the x direction (right/left) with projections along the y and z directions. Localization along this direction enabled separation of the samples transferred with and without the device. The readout gradient duration was 100 ms, giving a spectral resolution of 10 Hz, with a spectral bandwidth of 543 Hz to include the resonances of both pyruvate and urea. For image reconstruction, the even and odd EPI lobe data were combined by the sum-of-squares method. The data were acquired using the following parameters: flip angle = 10°; TE = 140 ms; TR = 2 s. Although the amounts of HP material in each syringe were approximately equal, the signal at thermal equilibrium was also measured to compensate for any potential residual differences in the amount of HP sample in each syringe.

HP MR In Vivo Experiments

HP [^{13}C]urea in vivo rat experiments were performed using a balanced steady state free precession (bSSFP) sequence (13) to acquire a coronal image (projection along the anterior–posterior direction) following a protocol approved by our Institutional Animal Care and Use Committee. The experiments were repeated twice on the same animal, one with HP sample transferred in ambient field, the other transferred with this device, while keeping all the other parameters the same. [^{13}C]urea was polarized for 88 ± 1 min and transferred to the scanner within 7 s. A 2.5 mL of the 100 mM solution was injected into a rat through tail vein catheter over 12 s with image acquisition starting at 20 s after the beginning of the injection. The imaging parameters were as follows: flip angle = 60°; TR = 15 ms; matrix size = 140 × 70; field of view = 20 × 10 cm; sequential phase encoding.

RESULTS

Magnetic Field Tests

The simulated and measured magnetic field distributions within the solenoid are shown in Figure 3. Figure 3A corresponds to the larger prototype solenoid, while Figure 3B corresponds to the actual solenoid used in this device. The measured results were close to the simulated results, but slightly higher in the center, as shown in Figure 3A. Using the same simulation method, we calculated the magnetic field of the device to be > 50 G over a 6-cm central section, as shown in Figure 3B. Even though the magnetic field drops quickly at both ends, the field is relatively uniform in the 3-cm central section where HP media is usually placed. When holding the switch and keeping the electric current on for about 30 s (the sample transfer usually takes <10 s), the measured magnetic field remained constant, thereby demonstrating the stability of the device.

HP MR Tests

In the HP [^{13}C]urea phantom experiments, the [^{13}C]urea signal in both syringes is shown in one axial image (Fig. 4A). The SNR increase achieved by using this device was demonstrated by the ratio of image intensity. The results showed a significantly ($P = 0.012$) higher (1.9 ± 0.2) [^{13}C]urea signal using the device. The result of the control group demonstrated a small effect between syringe locations (+4%). However, this effect was much smaller than the experimental signal ratio (~1.9) and therefore does not alter the conclusion that SNR increased by about two-fold. Furthermore, this small effect in the control group failed to reach statistical significance ($P = 0.098$).

For the HP copolarization phantom experiments, spectroscopic imaging was acquired to distinguish the different compounds based on frequency, and the different samples transferred with and without the device based on spatial location. The spectra were analyzed for each resonance and each transfer approach (Fig. 4B). The data showed a significantly ($P = 0.002$) higher (1.9 ± 0.3) [^{13}C]urea signal intensity in the sample transferred with the device. [1-^{13}C]pyruvate signal intensity was slightly higher (1.1 ± 0.1); however, it failed to reach statistical significance ($P = 0.550$).

The results of the HP [^{13}C]urea in vivo experiment are shown in Figure 5, along with the corresponding image from a 3D bSSFP ^{1}H scan. The coronal ^{13}C image with

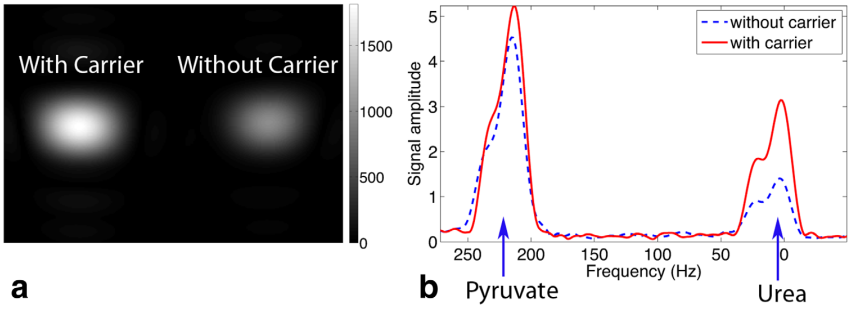

FIG. 4. Example of experimental comparisons between two HP samples scanned in one acquisition. One sample was transported with this device (with carrier), the other was transported in an ambient field (without carrier). The just urea experiment was performed using axial ^{13}C MRI (A), while the copolarization of urea and pyruvate MR spectroscopic imaging experiment resulted in two spectral peaks corresponding to the two HP compounds acquired from the samples transported with (solid red line) and without (dotted blue line) the carrier device (B). For copolarization results, the left peak corresponds to pyruvate and the right peak corresponds to urea. The center frequency was set close to the urea frequency.

sample transferred with the device has improved SNR. Quantitatively measuring the SNR at the center of the right kidney showed an SNR improvement of 1.8-fold with this device.

DISCUSSION

This device enabled a nearly 1.9-fold SNR improvement of HP urea signal compared with samples carried in the ambient field in HP [^{13}C]urea experiments, HP urea and pyruvate copolarization experiments, and one in vivo experiment. The observed 1.8- to 1.9-fold SNR improvement from experiments is close to the expected 1.83-fold increase predicted by simulation, which indicates that the hypothesis of fast signal decay due to scalar coupling relaxation is correct and that the model we use (Eq. 1) is accurate. Therefore, this model can be used for further study with other HP molecules. The SNR improvement may be even more significant in cases where the ambient field along transfer path is lower than in our facility.

Although [1-^{13}C]pyruvate is not affected by scalar coupling relaxation, other relaxation mechanisms could affect it at low fields, such as relaxation via paramagnetic centers (radical and gadolinium in solution). However, in our copolarization experiments, the [1-^{13}C]pyruvate signal was not significantly different with or without the device. Theoretically, the effect of relaxation via paramagnetic centers is small due to very low concentration of radical or gadolinium in the liquid state (16,17). Furthermore, this possible mechanism would likely have a small effect considering the transfer time is just 6 s, as a small fraction of expected T1 value (18). However, use of this device would prevent pyruvate relaxation effects that could occur at very low fields at some locations.

While the initial testing was focused on HP [^{13}C]urea and [1-^{13}C]pyruvate, it could also benefit other compounds. For example, HP [5-^{13}C]glutamine is being developed as a noninvasive imaging marker for

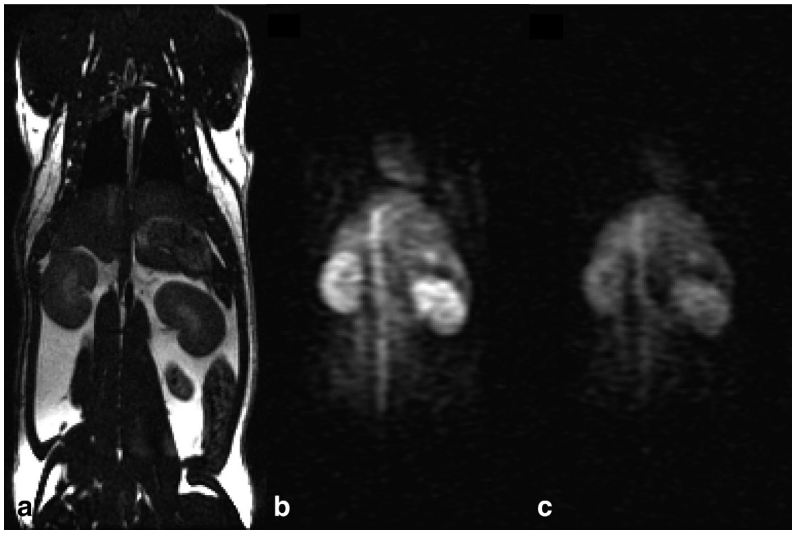

FIG. 5. In vivo rat experiment results. **A:** Coronal slice of a 3D bSSFP ^{1}H sequence. **B:** HP [^{13}C]urea image using a two-dimensional (coronal) bSSFP sequence (projection along the anterior–posterior direction) with sample transferred with the device. **C:** The same acquisition repeated on the same animal and position, but with the sample transferred in an ambient field. Images B and C were acquired with the same imaging parameters and experimental setup and differed only in the transfer method. Images B and C are displayed with the same window. The SNR (measured at right kidney center) in image B was 1.8 times higher using the device than without (image C).

glutaminolysis, allowing improved diagnosis and monitoring of glutamine-dependent tumors (19–21). Similar to urea, this substrate is also affected by coupling between ^{13}C and ^{14}N.

CONCLUSION

An electromagnet carrier device was designed and built to supply a suitable and safe magnetic field (>50 G) to preserve polarization during HP sample transfer, especially for compounds with scalar coupling between fast-relaxing quadrupolar ^{14}N and ^{13}C, such as in HP [^{13}C]urea. In comparative testing, this device demonstrated SNR improvements of approximately two-fold for [^{13}C]urea while maintaining the signal of HP [1-^{13}C]pyruvate.

ACKNOWLEDGMENTS

We thank Jeremy Bancroft Brown for assistance with 3D printing. We also thank Hsin-Yu Chen and Zihan Zhu for assistance with experiments.

REFERENCES

1. Ardenkjær-Larsen JH, Fridlund B, Gram A, Hansson G, Hansson L, Lerche MH, Servin R, Thaning M, Golman K. Increase in signal-to-noise ratio of >10,000 times in liquid-state NMR. Proc Natl Acad Sci U S A 2003;100:10158–10163.
2. Golman K, Ardenkjær-Larsen JH, Petersson JS, Månsson S, Leunbach I. Molecular imaging with endogenous substances. Proc Natl Acad Sci U S A 2003;100:10435–10439.
3. .Golman K, Thaning M. Real-time metabolic imaging. Proc Natl Acad Sci U S A 2006;103:11270–11275.
4. Chen AP, Albers MJ, Cunningham CH, et al. Hyperpolarized C-13 spectroscopic imaging of the TRAMP mouse at 3T-initial experience. Magn Reson Med 2007;58:1099–1106.
5. Nelson SJ, Kurhanewicz J, Vigneron DB, et al. Metabolic imaging of patients with prostate cancer using hyperpolarized [1-^{13}C] pyruvate. Sci Transl Med 2013;5:198ra108.
6. Chiavazza E, Kubala E, Gringeri CV, Düwel S, Durst M, Schulte RF, Menzel MI. Earth's magnetic field enabled scalar coupling relaxation of ^{13}C nuclei bound to fast-relaxing quadrupolar ^{14}N in amide groups. J Magn Reson 2013;227:35–38.
7. Kurhanewicz J, Vigneron DB, Brindle K, Chekmenev EY, Comment A, Cunningham CH, DeBerardinis RJ, Green GG, Leach MO, Rajan SS. Analysis of cancer metabolism by imaging hyperpolarized nuclei: prospects for translation to clinical research. Neoplasia 2011;13:81–97.
8. Johansson E, Månsson S, Wirestam R, Svensson J, Petersson J, Golman K, Ståhlberg F. Cerebral perfusion assessment by bolus tracking using hyperpolarized ^{13}C. Magn Reson Med 2004;51:464–472.
9. Svensson J, Månsson S, Johansson E, Petersson JS, Olsson LE. Hyperpolarized ^{13}C MR angiography using trueFISP. Magn Reson Med 2003;50:256–262.
10. Wilson DM, Keshari KR, Larson PEZ, Chen AP, Hu S, Criekinge MV, Bok R, Nelson SJ, Macdonald JM, Vigneron DB. Multi-compound polarization by DNP allows simultaneous assessment of multiple enzymatic activities *in vivo*. J Magn Reson 2010;205:141–147.
11. von Morze C, Larson PEZ, Hu S, Yoshihara HA, Bok RA, Goga A, Ardenkjaer-Larsen JH, Vigneron DB. Investigating tumor perfusion and metabolism using multiple hyperpolarized ^{13}C compounds: HP001, pyruvate and urea. Magn Reson Imaging 2012;30:305–311.
12. von Morze C, Bok RA, Sands JM, Kurhanewicz J, Vigneron DB. Monitoring urea transport in rat kidney in vivo using hyperpolarized ^{13}C magnetic resonance imaging. Am J Physiol Renal Physiol 2012;302:F1658–F1662.
13. Reed GD, von Morze C, Bok R, Koelsch BL, Van Criekinge M, Smith KJ, Shang H, Larson PEZ, Kurhanewicz J, Vigneron DB. High resolution C-13 MRI with hyperpolarized urea: in vivo T2 mapping and N-15 labeling effects. IEEE T Med Imaging 2014;33:362–371.
14. Lyerla JR Jr, Grant DM, Bertrand RD. Field-dependent contributions to carbon-13 nuclear relaxation. J Phys Chem 1971;75:3967–3971.
15. Cunningham CH, Chen AP, Albers MJ, Kurhanewicz J, Hurd RE, Yen Y-F, Pauly JM, Nelson SJ, Vigneron DB. Double spin-echo sequence for rapid spectroscopic imaging of hyperpolarized ^{13}C. J Magn Reson 2007;187:357–362.
16. Caravan P, Ellison JJ, McMurry TJ, Lauffer RB. Gadolinium(III) chelates as MRI contrast agents: structure, dynamics, and applications. Chem Rev 1999;99:2293–2352.
17. Gordon JW, Fain SB, Rowland IJ. Effect of lanthanide ions on dynamic nuclear polarization enhancement and liquid-state T1 relaxation. Magn Reson Med 2012;68:1949–1954.
18. Chattergoon N, Martinez-Santiesteban F, Handler WB, Ardenkjaer-Larsen JH, Scholl TJ. Field dependence of T_1 for hyperpolarized [1-^{13}C]pyruvate. Contrast Media Mol Imaging 2013;8:57–62.
19. Gallagher FA, Kettunen MI, Day SE, Lerche M, Brindle KM. ^{13}C MR spectroscopy measurements of glutaminase activity in human hepatocellular carcinoma cells using hyperpolarized ^{13}C-labeled glutamine. Magn Reson Med 2008;60:253–257.
20. Keshari KR, Wilson DM. Chemistry and biochemistry of ^{13}C hyperpolarized magnetic resonance using dynamic nuclear polarization. Chem Soc Rev 2014;43:1627–1659.
21. Daye D, Wellen KE. Metabolic reprogramming in cancer: unraveling the role of glutamine in tumorigenesis. Semin Cell Dev Biol 2012;23:362–369.